Journal of the Optical Society of Korea, Vol. 8, No. 3, September 2004, pp. 137-146

Eigenmode of Anisotropic Planar Waveguide

Gyeong-il Kweon*, Seung Hwang-bo, and Cheol-ho Kim

Department of Optoelectronics, Honam University
59-1, Seobong-dong, Gwangsan-gu, Gwangju, 506-714, KOREA

(Received March 11, 2004)

A new method of obtaining the eigenmode of an anisotropic planar waveguide is studied. The planar waveguide can be composed of an arbitrary number of isotropic or uniaxially anisotropic layers, provided all the optical axes are lying in the incidence plane. Since the equation of motion for the TE mode is not different from that for the TE mode in an isotropic planar waveguide, only the equation of motion for the TM mode is of any concern. For this kind of device structure, the Maxwell's equations can be solved for one component of the electric field and one component of the magnetic field. The resulting coupled set of equations is linear in the propagation constant and the eigenmode can be easily obtained using canned numerical routines.

OCIS codes : 230.7390,160.1190

I. INTRODUCTION

Birefringence in optical waveguides may or may not be a desirable aspect of the device. Polarization mode filters and polarizers have been successfully realized using an anisotropic substrate or a birefringent cladding [1-3]. Using a similar mechanism, an active device such as an amplitude modulator has been realized [4,5]. TE-TM mode converter is another polarization sensitive device which can benefit from the optical anisotropy [6,7]. Also, many interesting devices are based on $LiNbO_3$ where the optical birefringence is natural[8-11] or on GaAs or GaP where the birefringence can be electrically induced [12]. Crystal Quartz or Sapphire plate can be used as the substrate material for fabricating integrated optic devices. Furthermore, recent interest in photonic crystal waveguide necessitates taking the form birefringence into consideration [13]. Therefore, there are many incidences where optical anisotropy needs to be considered in analyzing device operation.

However, the modes of birefringent optical waveguides are considerably complicated and semi-analytic solutions have been obtained only for relatively simple geometries [14-27]. This semi-analytic approach is difficult to be generalized to more complex and potentially interesting structures. Even for a simple three-slab waveguide with one layer having an optical anisotropy, the semi-analytic solution yields a complicated transcendental equation that has to be solved for the zeros of a function.

More general solutions have been obtained using the transfer-matrix method [28-32]. This method is very general in that the orientation of the optical axis in each layer can be arbitrary and even the magnetically active layer can be incorporated. However, it is cumbersome in that the functional form of the mode has to be supplied and therefore the leaky or radiation mode has to be solved separately from the guided mode. Applying this method to a more general structure such as the gradient index waveguide would be an exhausting endeavor.

In another perspective, the Beam Propagation Method (BPM) has become a very important tool in understanding and designing optical devices including couplers, splitters, filters, spot size transformers, etc [33-41]. To initiate the BPM, an electromagnetic field profile has to be supplied which is usually chosen between the exact eigenmode or a Gaussian field profile. The choice of Gaussian beam often requires longer propagation length to stabilize the electric field. Because it is not trivial to obtain an eigenmode of an anisotropic waveguide, a Gaussian beam or other approximate eigenmode has often been used in the BPM analysis. Since the beam propagation method is based on finite-difference or finite elements meshes, it is desirable to have an eigenmode in the same meshes where the BPM is applied. Therefore there is still a need to obtain an eigenmode in finite-difference meshes.

In this article, we report a method of obtaining the numerical solution of an anisotropic planar waveguide for the case where the optical axis is lying in the

incidence plane [42]. The more general case of arbitrary optical axis orientation can be solved in a similar but more computationally intensive way.

II. LOCAL DIELECTRIC TENSOR

As schematically shown in Fig. 1, the coordinate system is chosen in such a way that the waveguide plane is parallel to the y-z plane and the mode is assumed to propagate along the positive z-axis. Because of the planar waveguide geometry, the dielectric permittivity tensor is a single function of position (i.e. $\varepsilon \equiv \varepsilon(x)$). We further require that the birefringence is limited to uniaxial anisotropy with the optical axis lying in the incidence plane (x-z plane), and consequently there is no mixing between ordinary and extraordinary waves.

The local dielectric tensor for the uniaxial optical anisotropy within its own principal axis coordinate system becomes diagonal.

$$\varepsilon'(x)=\begin{pmatrix}\varepsilon_1(x) & 0 & 0\\ 0 & \varepsilon_1(x) & 0\\ 0 & 0 & \varepsilon_3(x)\end{pmatrix}. \tag{1}$$

The dielectric tensor in the laboratory coordinate system is related to the dielectric tensor in the principal axis coordinate system by a rotation matrix R given as

$$R(x)=\begin{pmatrix}\cos\alpha(x) & 0 & -\sin\alpha(x)\\ 0 & 1 & 0\\ \sin\alpha(x) & 0 & \cos\alpha(x)\end{pmatrix}, \tag{2}$$

where α is the angle formed by the z-axis and the local optical axis (i.e. c-axis) at position x. Then the local dielectric tensor in the laboratory frame is given as

$$\varepsilon(x)=R^T(x)\varepsilon'(x)R(x), \tag{3}$$

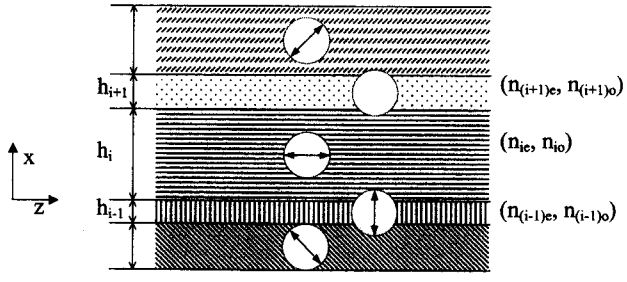

FIG. 1. Schematic diagram of an anisotropic multilayer planar waveguide. Each layer can be either isotropic layer or a uniaxially-anisotropic layer with the optical axis lying in the x-z plane.

where $R^T(x)$ is the transpose matrix of $R(x)$. Upon the evaluation of the matrix multiplication, the dielectric tensor in the laboratory coordinate frame is found as [18]

$$\varepsilon=\begin{pmatrix}\varepsilon_{xx} & 0 & \varepsilon_{xz}\\ 0 & \varepsilon_{yy} & 0\\ \varepsilon_{xz} & 0 & \varepsilon_{zz}\end{pmatrix}, \tag{4}$$

where the dependence on the position x has been suppressed for the simplicity of notation. The matrix elements in Eq. (4) are given as

$$\varepsilon_{xx}=\varepsilon_1\cos^2\alpha+\varepsilon_3\sin^2\alpha, \tag{5}$$

$$\varepsilon_{xz}=(\varepsilon_3-\varepsilon_1)\sin\alpha\cos\alpha, \tag{6}$$

$$\varepsilon_{zz}=\varepsilon_1\sin^2\alpha+\varepsilon_3\cos^2\alpha, \tag{7}$$

and

$$\varepsilon_{yy}=\varepsilon_1. \tag{8}$$

It can be easily checked that the inverse matrix is given as

$$\varepsilon^{-1}=\frac{1}{\eta}\begin{pmatrix}\varepsilon_{zz} & 0 & -\varepsilon_{xz}\\ 0 & \dfrac{\eta}{\varepsilon_{yy}} & 0\\ -\varepsilon_{xz} & 0 & \varepsilon_{xx}\end{pmatrix}, \tag{9}$$

where

$$\eta=\varepsilon_{xx}\varepsilon_{zz}-\varepsilon_{xz}^2. \tag{10}$$

III. FORMALISM

Assuming a harmonic time dependence ($\propto \exp[j\omega t]$), the modified Ampere's law in source free region is given as

$$\nabla\times\boldsymbol{H}(\boldsymbol{r},t)=j\omega\varepsilon(\boldsymbol{r},t)\boldsymbol{E}(\boldsymbol{r},t), \tag{11}$$

and Faraday's law is given as

$$\nabla\times\boldsymbol{E}(\boldsymbol{r},t)=-j\omega\mu\boldsymbol{H}(\boldsymbol{r},t), \tag{12}$$

where $\boldsymbol{E}(\boldsymbol{r},t)$ is the electric field vector at position $\boldsymbol{r}$ and time t. $\boldsymbol{H}(\boldsymbol{r},t)$ is the magnetic field vector, ω the angular frequency of the field, and μ the magnetic permeability of the vacuum.

We limit our interest to extraordinary waves only. The behavior of ordinary waves in this waveguide structure is not different from that of ordinary scalar dielectric permittivity [18], provided we identify the scalar dielectric permittivity with $\varepsilon_{yy}=\varepsilon_1$. Extraor-

dinary waves in this structure correspond to transverse magnetic (TM) modes, and the electric and magnetic fields are given as

$$\boldsymbol{E}(\boldsymbol{r},t)=\begin{pmatrix}E_x(\boldsymbol{r},t)\\0\\E_z(\boldsymbol{r},t)\end{pmatrix}=\exp[j(\omega t-\beta z)]\begin{pmatrix}E'_x(x)\\0\\E'_z(x)\end{pmatrix}, \tag{13}$$

$$\boldsymbol{H}(\boldsymbol{r},t)=\begin{pmatrix}0\\H_y(\boldsymbol{r},t)\\0\end{pmatrix}=\exp[j(\omega t-\beta z)]\begin{pmatrix}0\\H'_y(x)\\0\end{pmatrix}, \tag{14}$$

where β is the propagation constant. Then from Eqs. (9) and (11), it can be shown that

$$E'_x=\frac{j}{\omega\eta}\left[\varepsilon_{xx}\frac{\partial H'_y}{\partial x}-j\beta\varepsilon_{zz}H'_y\right], \tag{15}$$

and

$$E'_z=-\frac{j}{\omega\eta}\left[\varepsilon_{xx}\frac{\partial H'_y}{\partial x}-j\beta\varepsilon_{zz}H'_y\right]. \tag{16}$$

For the TM modes in planar waveguides, the characteristic equation is obtained by taking the curl of Eq. (11) and using the relation in Eq. (12) to eliminate the electric field.

$$\nabla\times\left(\varepsilon^{-1}\nabla\times\boldsymbol{H}\right)=\omega^2\mu\boldsymbol{H}. \tag{17}$$

In an ordinary planar waveguide without any optical anisotropy, this equation is reduced to

$$\varepsilon\frac{\partial}{\partial x}\left(\frac{1}{\varepsilon}\frac{\partial H'_y}{\partial x}\right)=\left(\beta^2-k_o^2\frac{\varepsilon}{\varepsilon_o}\right)H'_y, \tag{18}$$

where k_o is the wave number in free space, and ε_o is the dielectric permittivity of the vacuum. On the other hand, however, Eq. (17) in the present anisotropic planar waveguide is reduced to

$$\omega^2\mu H'_y+\frac{\partial}{\partial x}\left(\frac{\varepsilon_{xx}}{\eta}\right)\frac{\partial H'_y}{\partial x}+\frac{\varepsilon_{xx}}{\eta}\frac{\partial^2 H'_y}{\partial x^2}$$
$$=\beta^2\frac{\varepsilon_{zz}}{\eta}H'_y+j2\beta\frac{\varepsilon_{zz}}{\eta}\frac{\partial H'_y}{\partial x}+j\beta\frac{\partial}{\partial x}\left(\frac{\varepsilon_{zz}}{\eta}\right)H'_y. \tag{19}$$

This is a non-linear equation for the propagation constant β and consequently the solution cannot be easily obtained from the usual eigenvector analysis.

Another approach takes the curl of Eq. (12), and the resulting equation is given as

$$\nabla^2\boldsymbol{E}-\nabla(\nabla\cdot\boldsymbol{E})+\omega^2\mu\varepsilon\boldsymbol{E}=0. \tag{20}$$

Using Eq. (15), this equation is reduced to a set of coupled non-linear equations of the propagation constant.

$$\omega^2\mu\varepsilon_{xx}E'_x+\omega^2\mu\varepsilon_{xx}E'_z=\beta^2E'_x-j\beta\frac{\partial E'_z}{\partial x}, \tag{21}$$

and

$$\omega^2\mu\varepsilon_{xx}E'_x+\frac{\partial^2E'_z}{\partial x^2}+\omega^2\mu\varepsilon_{zz}E'_z=-j\beta\frac{\partial E'_x}{\partial x}. \tag{22}$$

Therefore this equation is no easier to solve than Eq. (19).

The most convenient solution is obtained by using the two first order equations (11) and (12), and eliminating one component of the electric field (E_z) by using the relation in Eq. (16). The resulting coupled equations are given as

$$\left\{-j\frac{\partial}{\partial x}\left(\frac{\varepsilon_{xx}}{\varepsilon_{zz}}\right)-j\frac{\varepsilon_{xx}}{\varepsilon_{zz}}\frac{\partial}{\partial x}\right\}E'_x$$
$$+\left\{\omega\mu+\frac{1}{\omega}\frac{\partial}{\partial x}\left(\frac{1}{\varepsilon_{zz}}\right)\frac{\partial}{\partial x}+\frac{1}{\omega\varepsilon_{zz}}\frac{\partial^2}{\partial x^2}\right\}H'_y=\beta E'_x, \tag{23}$$

and

$$\omega\left(\varepsilon_{xx}-\frac{\varepsilon_{xx}^2}{\varepsilon_{zz}}\right)E'_x-j\frac{\varepsilon_{xx}}{\varepsilon_{zz}}\frac{\partial H'_y}{\partial x}=\beta H'_y. \tag{24}$$

By renormalizing the electric and magnetic fields, the coupled equations are given as

$$\begin{pmatrix}-j\frac{\partial}{\partial\tilde{x}}\left(\frac{\tilde{\varepsilon}_{xx}}{\tilde{\varepsilon}_{zz}}\right)-j\frac{\tilde{\varepsilon}_{xx}}{\tilde{\varepsilon}_{zz}}\frac{\partial}{\partial\tilde{x}} & \tilde{k}_o^2+\frac{\partial}{\partial\tilde{x}}\left(\frac{1}{\tilde{\varepsilon}_{zz}}\right)\frac{\partial}{\partial\tilde{x}}+\frac{1}{\tilde{\varepsilon}_{zz}}\frac{\partial^2}{\partial\tilde{x}^2}\\ \tilde{\varepsilon}_{xx}-\frac{\tilde{\varepsilon}_{xx}^2}{\tilde{\varepsilon}_{zz}} & -j\frac{\tilde{\varepsilon}_{xx}}{\tilde{\varepsilon}_{zz}}\frac{\partial}{\partial\tilde{x}}\end{pmatrix}\begin{pmatrix}\tilde{E}'_x\\\tilde{H}'_y\end{pmatrix}=\tilde{\beta}\begin{pmatrix}\tilde{E}'_x\\\tilde{H}'_y\end{pmatrix}. \tag{25}$$

In Eq. (25), the distance is measured in micrometer units since the characteristic dimensions of a typical waveguide and the wavelength of interest are of the order of a micrometer.

$$\tilde{x}=\frac{x}{\mu m}. \tag{26}$$

Since the wavenumber has the dimension of an inverse distance, the normalized wavenumber is given as,

$$\tilde{k}_o=k_o\mu m. \tag{27}$$

On the other hand, the dielectric permittivity is measured in terms of the vacuum dielectric permittivity.

$$\tilde{\varepsilon}_{xx}=\frac{\varepsilon_{xx}}{\varepsilon_o}, \tag{28}$$

and similarly for other tensor components. The electric field is used as it is,

$$\tilde{E}'_x = E'_x, \tag{29}$$

while the magnetic field is normalized using a product of the micrometer distance, angular frequency and the vacuum dielectric permittivity.

$$\tilde{H}'_y = \frac{H'_y}{\mu m \omega \varepsilon_o}. \tag{30}$$

Eq. (25) is a set of coupled linear equations of the propagation constant and the eigenmode can be easily obtained by using the standard technique of eigenvector analysis. (The details of obtaining a numerical solution is given in the appendix.) The only drawback is with respect to the increased demand on the computer. If we could obtain a satisfactory finite-differencing solution of the ordinary planar waveguide using an N×N matrix, then we will at least need a 2N ×2N matrix to obtain a similar result for the anisotropic planar waveguide.

The most general anisotropic planar optical waveguide would allow the birefringence in each layer to be either uniaxial or biaxial and the orientation of the optical axis in each layer to be arbitrary. This structure can also be solved using a similar approach and the resulting coupled set of first order differential equations will be similar to the Berreman's 4×4 matrix [29,43,44]. Therefore to obtain an eigenmode with a precision comparable to that of an isotropic optical waveguide, we would need a 4N×4N matrix.

IV. EXAMPLES

Fig. 2 shows a schematic diagram of a simple device where an anisotropic crystal plate is assumed to be used as the substrate and the optical axis of the uniaxially anisotropic substrate makes an angle of ϕ with the propagation axis z. A core layer of thickness h and refractive index n_f is assumed to have been deposited on the substrate and air is used as the upper clad. Because of the simple structure, the eigenmode can be obtained both semi-analytically and numerically. Devices based on anisotropic substrate or cover can be analyzed using this model.

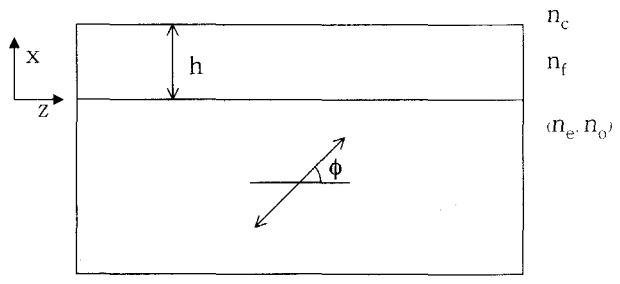

FIG. 2. Simple three-slab waveguide with isotropic core and cover and uniaxially anisotropic substrate.

In an isotropic medium, the equation of motion for the magnetic field is given by Eq. (18). Within the homogeneous film, this equation is further simplified to the familiar form given as

$$\frac{\partial^2 H'_y}{\partial x^2} + n_f^2 k_o^2 H'_y = \beta^2 H'_y. \tag{31}$$

Similar equation holds for the cover. On the other hand in the anisotropic substrate, the magnetic field satisfies Eq. (19) which can be rearranged as

$$\frac{\partial^2 H'_y}{\partial x^2} - 2i\frac{\varepsilon_{xz}}{\varepsilon_{xx}}\beta\frac{\partial H'_y}{\partial x} + \left[\frac{\eta k_o^2}{\varepsilon_o \varepsilon_{xx}} - \frac{\varepsilon_{zz}}{\varepsilon_{xx}}\beta^2\right] H'_y = 0. \tag{32}$$

The functional form of the magnetic field for the lowest order guided mode within the film can be easily written down as

$$H'_y(0 \le x \le h) = H_f \cos(\kappa_f x - \phi_s), \tag{33}$$

where H_f is the normalization constant and the transverse propagation constant κ_f is defined as [45]

$$\kappa_f^2 = n_f^2 k_o^2 - \beta^2. \tag{34}$$

Similarly the magnetic field in the cover is given as

$$H'_y(x \ge h) = H_f \cos(\kappa_f h - \phi_s)\exp[-\gamma_c(x-h)], \tag{35}$$

where the normalization constant in the cover has been chosen in such a way that the magnetic field is automatically continuous at the film-cover interface, and the transverse decay constant γ_c is defined as

$$\gamma_c^2 = \beta^2 - n_c^2 k_o^2. \tag{36}$$

The tangential component of the electric field in an isotropic medium is given in terms of the magnetic field as

$$E'_z = -\frac{i}{\omega\varepsilon}\frac{\partial H'_y}{\partial x}. \tag{37}$$

The continuity of the tangential component of the electric field at the film-cover interface results in a transcendental equation.

$$\frac{n_f^2 \gamma_c}{n_c^2 \kappa_f} = \tan(\kappa_f h - \phi_s). \tag{38}$$

Within the anisotropic substrate, the magnetic field can be written as

$$H_y'(x \le 0) = H_f \cos(\phi_s) \exp[(\gamma + i\rho)x], \tag{39}$$

where ρ and γ are defined as

$$\rho = \frac{\varepsilon_{xz}}{\varepsilon_{xx}}\beta, \tag{40}$$

and

$$\gamma^2 = \frac{\eta}{\varepsilon_{xx}^2}\left(\beta^2 - \frac{\varepsilon_{xx}}{\varepsilon_o}k_o^2\right). \tag{41}$$

Utilizing Eqs. (16) and (37), the continuity of the tangential component of the electric field at the film-substrate interface results in another transcendental equation given as

$$\frac{\gamma}{\kappa_f}\frac{\varepsilon_o n_f^2 \varepsilon_{xx}}{\eta} = \tan\phi_s. \tag{42}$$

Combining these two transcendental equations given in Eqs. (38) and (42), the dispersion relation for the device is given as

$$\tan(\kappa_f h) = \frac{\varepsilon_f \eta \kappa_f \gamma_c + \varepsilon_f \varepsilon_c \varepsilon_{xx} \kappa_f \gamma}{\varepsilon_c \eta \kappa_f^2 - \varepsilon_f^2 \varepsilon_{xx} \gamma \gamma_c}. \tag{43}$$

In the case of the isotropic substance (i.e. $\varepsilon_{xx} = \varepsilon_1 = \varepsilon_3 = \varepsilon_s$), the dispersion relation is reduced to a familiar form given as

$$\tan(\kappa_f h) = \frac{\left(\frac{\varepsilon_f}{\varepsilon_s}\right)\frac{\gamma_s}{\kappa_f} + \left(\frac{\varepsilon_f}{\varepsilon_c}\right)\frac{\gamma_c}{\kappa_f}}{1 - \left(\frac{\varepsilon_f}{\varepsilon_s}\right)\frac{\gamma_s}{\kappa_f}\left(\frac{\varepsilon_f}{\varepsilon_c}\right)\frac{\gamma_c}{\kappa_f}}. \tag{44}$$

Therefore the case of the three-slab waveguide with isotropic layers is a special example of a more general three-slab waveguide with anisotropic substrate or cover.

The parameters used in the numerical analysis are as follows. The extra-ordinary (n_e) and ordinary (n_o) refractive indices are assumed as 1.466 and 1.577, respectively. These are the refractive indices of Calcite at 1.55 μm. The inclination of the optical axis is assumed as $\pi/3$ (60°), and the film (core) refractive index is assumed as the same as n_o, and the film thickness is assumed as 3 μm. Fig. 3 shows the dielectric permittivity distribution of the waveguide for the chosen parameter sets. The film-substrate boundary is located at $x = 0$ μm and the film-cover boundary at $x = 3$ μm.

Fig. 4 shows the dispersion relation given in Eq. (43) as a function of the effective refractive index of the waveguide. Curve a is the left-hand side (LHS) of Eq. (43), while curve b is the right-hand side of the equation. The two curves are shown only where their values are real. From the graph, we can see that this structure has only one guided mode.

Fig. 5 shows the fundamental mode of the three-slab waveguide calculated by the semi-analytical method (curve a: dotted line) and the numerical method (curve b: solid line). In the numerical method, a computational window of 15 μm width has been discretized with 2^8 points. The locations of the film-substrate and film-cover interfaces are marked with vertical lines. Due to the large difference in the refractive indices, the field intensity in the air cover is minimal while it

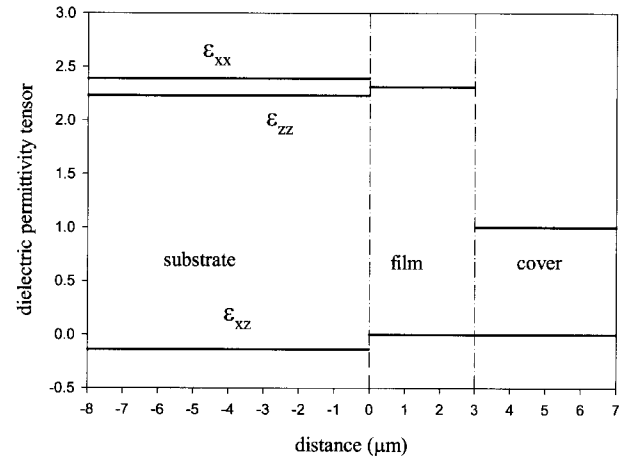

FIG. 3. The dielectric permittivity distribution for the three-slab waveguide.

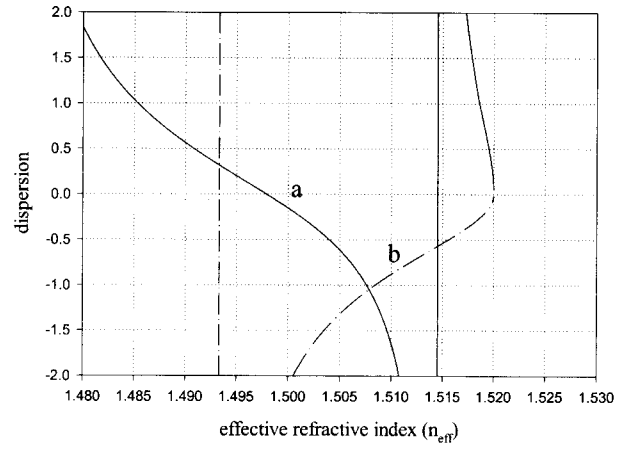

FIG. 4. Dispersion relation for the three-slab waveguide depicted in Fig. 2. Curves a and b correspond to the LHS (Left Hand Side) and RHS (Right Hand Side) of Eq. (43).

penetrates substantial distance into the substrate. Fig. 6 shows the electric field amplitude as a function of two space variables x and z. Wave front in the substrate at the lower part of the graph is clearly skewed toward the film as has been pointed out in ref. 18.

Fig. 7 shows the effective refractive indices of the guided mode as a function of the angle ϕ between the z-axis and optical axis. The effective refractive index of the guided mode is calculated by both the semi-analytical method and the numerical method. The graph is symmetric about the center indicating that the propagation constant is independent of the sign of the angle ϕ. When $|\phi| \approx \pi/2$, the waveguide supports two guided modes. From the graph, the two effective refractive indices calculated by the two method are almost indistinguishable for the fundamental mode but shows slight difference for the first order mode at the lower part of the graph.

From these results, it is confirmed that the numerical solution agrees well with the semi-analytical solution for the simple structures. The numerical algorithm, however, can be applied to structures where the semi-analytical solution is difficult to obtain. For example, a graded-index type anisotropic waveguide can be envisaged. Core in $LiNbO_3$-based optical waveguide is usually fabricated by metal diffusion. Therefore core and clad are both optically anisotropic and the dielectric permittivity is a continuous function of position. The current formalism extended to quasi-TE mode can be applied for such structure. For our planar waveguide example, we will consider an anisotropic waveguide where the local optical axis changes its direction continuously. Specifically we assume the same ordinary and extra-ordinary refractive indices as in the previous example, but the angle ϕ is given as a continuous function of position x (i.e. ϕ = arctangent (x)). Separate cover and substrate are not needed for this waveguide. Fig. 8 shows the dielectric permittivity distribution for this structure. This waveguide has some similarity with liquid crystals where the orientation of the liquid crystal molecule changes continuously when properly biased. The structure we are considering is not found naturally. However, rapid development of lithographic technology enables many remarkable structures to be realized. If we fabricate a grating structure where the line and space is much smaller than the wavelength of

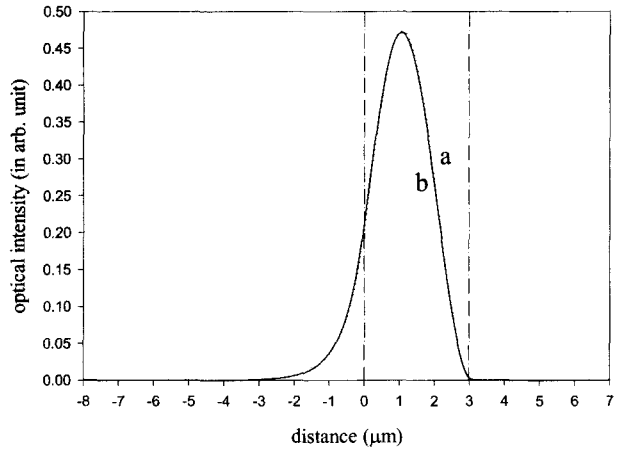

FIG. 5. The fundamental mode of the waveguide calculated by the semi-analytical method (curve a: dotted curve) and the numerical method (curve b: solid curve). Two vertical lines denote the boundaries between the substrate-core and core-cover, respectively.

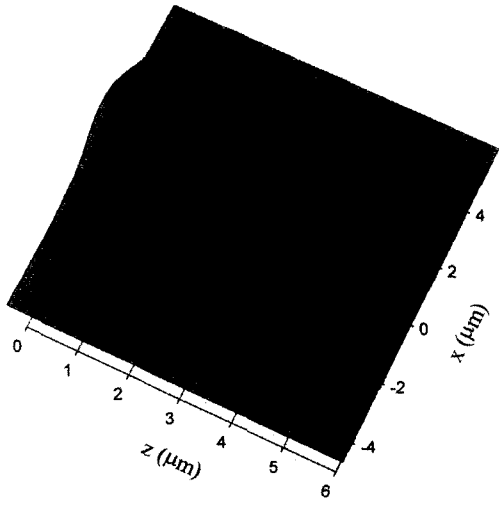

FIG. 6. Electromagnetic field profile of the fundamental mode of the waveguide as a function of x and z coordinates. In the cover (upper part of the figure), the field amplitude is minimal due to the large difference in the refractive indices. In the anisotropic substrate, the wave front is skewed as is described in ref. 18.

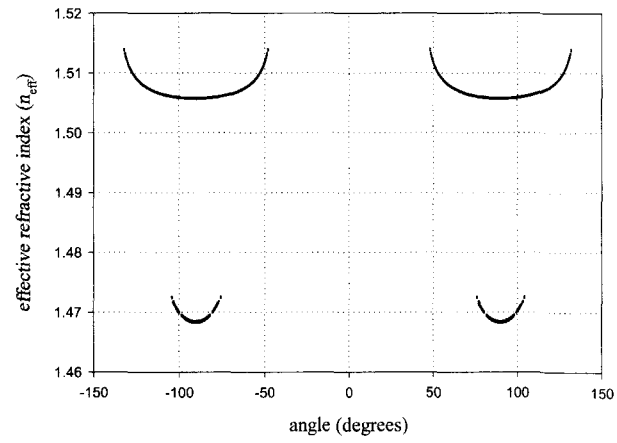

FIG. 7. Effective refractive indices of the guided modes of the three-slab waveguide. The angle ϕ between the waveguide axis (i.e. z-axis) and the optical axis is varied, while all the other parameters are kept the same as in the preceding figures.

interest, then the light does not feel the structural details, and the structure appears as an anisotropic homogeneous medium, a phenomenon known as form birefringence. Photonic crystal waveguide inevitably induces form birefringence, which can be either desirable or not desirable depending on the intent of the designer. At any rate, this graded-index type waveguide may be realized by fabricating deeply etched narrow gratings where the line and space are much smaller than the wavelength of interest and the line and space are continuously curved so that each line appears as an arctangent line. Fig. 9 shows the intensity profile of the fundamental mode along with the ε_{xx} component of the dielectric permittivity for size comparison. The number of discretization points is the same as that of Fig. 5.

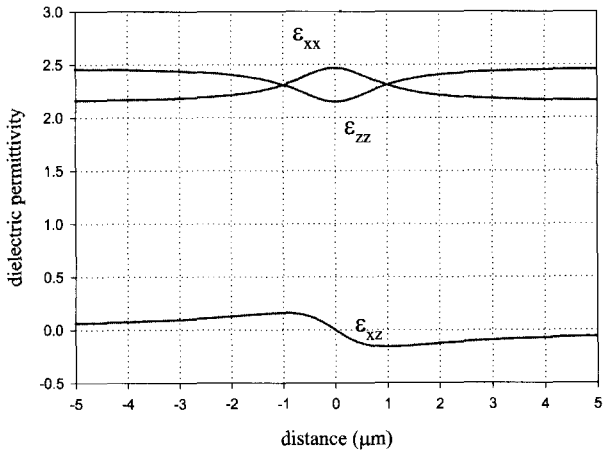

FIG. 8. Dielectric permittivity of a graded-index type anisotropic planar waveguide. The ordinary and extraordinary refractive indices are those of a Calcite at 1550 nm. The angle between the z-axis and the optical axis is given as an arctangent function of x.

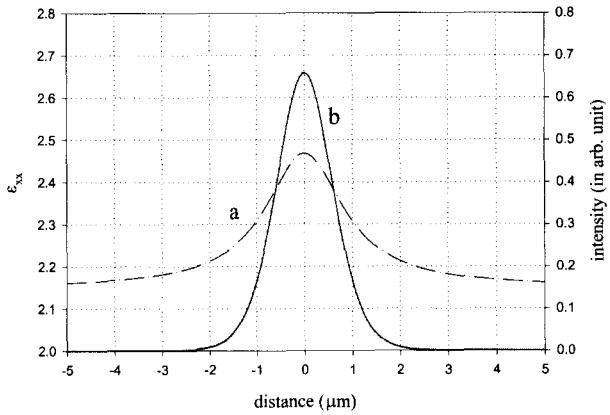

FIG. 9. Curve a is the ε_{xx} component of the dielectric permittivity and curve b is the intensity profile of the lowest order guided (i.e., fundamental) mode.

V. CONCLUSIONS

In conclusion, we have shown that general eigenmodes of anisotropic planar waveguides with the uniaxially-anisotropic optical axis lying in the incidence plane can be numerically solved using two first-order equations involving both electric and magnetic fields.

*Corresponding author : kweon@honam.ac.kr

APPENDIX

The renormalized eigenmode equation for a TM mode is given as

$$\begin{pmatrix} -j\dfrac{\partial}{\partial\tilde{x}}\left(\dfrac{\tilde{\varepsilon}_{xz}}{\tilde{\varepsilon}_{zz}}\right)-j\dfrac{\tilde{\varepsilon}_{xz}}{\tilde{\varepsilon}_{zz}}\dfrac{\partial}{\partial\tilde{x}} & \tilde{k}_0^2+\dfrac{\partial}{\partial\tilde{x}}\left(\dfrac{1}{\tilde{\varepsilon}_{zz}}\right)\dfrac{\partial}{\partial\tilde{x}}+\dfrac{1}{\tilde{\varepsilon}_{zz}}\dfrac{\partial^2}{\partial\tilde{x}^2} \\ \tilde{\varepsilon}_{xx}-\dfrac{\tilde{\varepsilon}_{xz}^2}{\tilde{\varepsilon}_{zz}} & -j\dfrac{\tilde{\varepsilon}_{xz}}{\tilde{\varepsilon}_{zz}}\dfrac{\partial}{\partial\tilde{x}} \end{pmatrix}\begin{pmatrix}\tilde{E}_x' \\ \tilde{H}_y'\end{pmatrix}=\tilde{\beta}\begin{pmatrix}\tilde{E}_x' \\ \tilde{H}_y'\end{pmatrix}. \tag{A1}$$

For an illustrative purpose, we will solve this equation using a uniform finite-differencing scheme [46,47]. As schematically shown in Fig. 10, a computational window with a width of *window* μm is set-up. The width and the location of the window is such that the region of the waveguide of interest is near the center of the computational window and all the possible guided modes does not significantly extend beyond the rim of the computational window. The proper width of the computational window depends on how strongly or weakly guiding the waveguide is. Although, the location of the origin can be anywhere, even outside the computational window, we will assume for simplicity of notation that the origin of the coordinate coincides with the left end of the computational window. Then the x-variable extends from x = 0 to x = *window*.

This computational window is uniformly divided into (L_{max} - 1) equal intervals, where $N = L_{max}$ is usually chosen as a power of 2, for example $N = 2^8$ for the Figs.

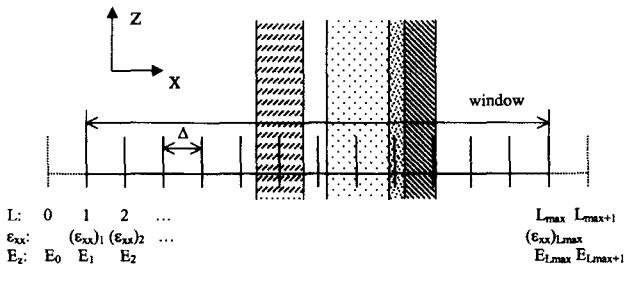

FIG. 10. Schematic diagram illustrating a uniform finite-differencing scheme.

5 and 9. Then each interval is of a width given as $\triangle$ = *window* / (L_{max} - 1), and the discretized x-variable has L_{max} components as given by x_1, x_2, $\cdots$ x_{L-1}, x_L, x_{L+1}, $\cdots x_{Lmax}$. The magnitude of x_L is simply given as $x_L = \triangle(L - 1)$. To apply the boundary conditions, two extra points are assigned just outside the computational window (i.e., $x_o = -\triangle$, $x_{Lmax+1} = x_{Lmax} + \triangle = \triangle L_{max}$). The discretized dielectric tensor ε_{xx} and the electric field at $x = x_L$ are denoted as $(\varepsilon_{xx})_L$ and E_L, respectively.

In this simple uniform differencing scheme, the coupled set of equations in Eq. (A1) are given as

$$-\frac{j}{2\Delta}\left\{\left(\frac{\tilde{\varepsilon}_{xz}}{\tilde{\varepsilon}_{zz}}\right)_{L+1}-\left(\frac{\tilde{\varepsilon}_{xz}}{\tilde{\varepsilon}_{zz}}\right)_{L-1}\right\}\left(\tilde{E}'_x\right)_L-\frac{j}{2\Delta}\left(\frac{\tilde{\varepsilon}_{xz}}{\tilde{\varepsilon}_{zz}}\right)_L\left(\tilde{E}'_x\right)_{L+1}+\frac{j}{2\Delta}\left(\frac{\tilde{\varepsilon}_{xz}}{\tilde{\varepsilon}_{zz}}\right)_L\left(\tilde{E}'_x\right)_{L-1}$$
$$+\left\{k_o^2-\frac{2}{\Delta^2}\left(\frac{1}{\tilde{\varepsilon}_{zz}}\right)_L\right\}\left(\tilde{H}'_y\right)_L+\frac{1}{\Delta^2}\left\{\left(\frac{1}{\tilde{\varepsilon}_{zz}}\right)_L+\frac{1}{4}\left(\frac{1}{\tilde{\varepsilon}_{zz}}\right)_{L+1}-\frac{1}{4}\left(\frac{1}{\tilde{\varepsilon}_{zz}}\right)_{L-1}\right\}\left(\tilde{H}'_y\right)_{L+1}$$
$$+\frac{1}{\Delta^2}\left\{\left(\frac{1}{\tilde{\varepsilon}_{zz}}\right)_L-\frac{1}{4}\left(\frac{1}{\tilde{\varepsilon}_{zz}}\right)_{L+1}+\frac{1}{4}\left(\frac{1}{\tilde{\varepsilon}_{zz}}\right)_{L-1}\right\}\left(\tilde{H}'_y\right)_{L-1}=\beta\left(\tilde{E}'_x\right)_L, \tag{A2}$$

and

$$\left\{(\tilde{\varepsilon}_{xx})_L-\left(\frac{\tilde{\varepsilon}_{xz}^2}{\tilde{\varepsilon}_{zz}}\right)_L\right\}\left(\tilde{E}'_x\right)_L-\frac{j}{2\Delta}\left(\frac{\tilde{\varepsilon}_{xz}}{\tilde{\varepsilon}_{zz}}\right)_L\left(\tilde{H}'_y\right)_{L+1}+\frac{j}{2\Delta}\left(\frac{\tilde{\varepsilon}_{xz}}{\tilde{\varepsilon}_{zz}}\right)_L\left(\tilde{H}'_y\right)_{L-1}=\beta\left(\tilde{H}'_y\right)_L. \tag{A3}$$

There are a total of L_{max} equations of (A2) form and another L_{max} equations of (A3) form. These $2L_{max}$ equations can be arranged in a matrix equation as given by

$$[A]\vec{V}=\beta\vec{V}, \tag{A4}$$

where [A] is a characteristic square ($2L_{max} \times 2L_{max}$) matrix and $\vec{V}$ is a column vector ($2L_{max} \times 1$) given as,

$$V_L=\left(\tilde{E}'_x\right)_L, \tag{A5}$$

and

$$V_{L\max+L}=\left(\tilde{H}'_y\right)_L. \tag{A6}$$

When L is either 1 or L_{max}, non-physical quantities such as E_o, $(\varepsilon_{xx})_o$, or E_{Lmax+1}, $(\varepsilon_{xx})_{Lmax+1}$ appear in Eqs. (A2) and (A3). Then either Dirichlet or Neumann boundary conditions can be used to eliminate such quantities. When Neumann boundary condition is used, for example, then the physical quantity at the rim of the computational window is assumed as uniform (i.e., derivative is zero). Therefore the unphysical quantities at the outside of the computational window are replaced by the values of their nearest neighbor (i.e., $E_o = E_1$, $(\varepsilon_{xx})_o = (\varepsilon_{xx})_1$, $E_{Lmax+1} = E_{Lmax}$ and etc). When the waveguide is weakly guiding or leaky, various artificial boundaries can be added such as the perfectly matched layer (PML) boundary condition [48]. Following is a sample *MatLab* code defining the characteristic matrix in Eq. (A4).

```
A = zeros(2 * Lmax, 2 * Lmax);
A(1, 1) = - j / (2 * dX) * (exz(2) / ezz(2) - 2 * exz(1) / ezz(1));
A(1, 2) = - j / (2 * dX) * (exz(1) / ezz(1));
A(1, Lmax + 1) = ko ^ 2 - 1 / (4 * dX ^ 2) * (1 / ezz(2) + 3 /
ezz(1));
A(1, Lmax + 2) = 1 / (4 * dX ^ 2) * (1 / ezz(2) + 3 / ezz(1));
%
for L = 2: Lmax - 1
    A(L, L - 1) = j / (2 * dX) * (exz(L) / ezz(L));
    A(L, L) = - j / (2 * dX) * (exz(L + 1) / ezz(L + 1) - exz(L
    - 1) / ezz(L - 1));
    A(L, L + 1) = - j / (2 * dX) * (exz(L) / ezz(L));
    A(L, Lmax + L - 1) = 1 / (4 * dX ^ 2) ...
            * (- 1 / ezz(L + 1) + 4 / ezz(L) + 1 / ezz(L - 1));
    A(L, Lmax + L) = ko ^ 2 - 2 / dX ^ 2 * (1 / ezz(L));
    A(L, Lmax + L + 1) = 1 / (4 * dX ^ 2) * (1 / ezz(L + 1) +
    4 / ezz(L) - 1 / ezz(L - 1));
end
A(Lmax, Lmax - 1) = j / (2 * dX) * (exz(Lmax) / ezz(Lmax));
A(Lmax, Lmax) = - j / (2 * dX) ...
            * (2 * exz(Lmax) / ezz(Lmax) - exz(Lmax - 1) /
              ezz(Lmax - 1));
A(Lmax, 2 * Lmax - 1) = 1 / (4 * dX ^ 2) * (3 / ezz(Lmax) + 1
/ ezz(Lmax - 1));
A(Lmax, 2 * Lmax) = ko ^ 2 - 1 / (4 * dX ^ 2) * (3 / ezz(Lmax)
+ 1 / ezz(Lmax - 1));
A(Lmax + 1, 1) = exx(1) - (exz(1)) ^ 2 / ezz(1);
A(Lmax + 1, Lmax + 1) = j / (2 * dX) * exz(1) / ezz(1);
A(Lmax + 1, Lmax + 2) = - j / (2 * dX) * exz(1) / ezz(1);
for L = 2: Lmax - 1
    A(Lmax + L, L) = exx(L) - (exz(L)) ^ 2 / ezz(L);
    A(Lmax + L, Lmax + L - 1) = j / (2 * dX) * exz(L) / ezz(L);
    A(Lmax + L, Lmax + L + 1) = - j / (2 * dX) * exz(L) / ezz(L);
end
A(2 * Lmax, Lmax) = exx(Lmax) - (exz(Lmax)) ^ 2 / ezz(Lmax);
A(2 * Lmax, 2 * Lmax - 1) = j / (2 * dX) * exz(Lmax) / ezz(Lmax);
A(2 * Lmax, 2 * Lmax) = - j / (2 * dX) * exz(Lmax) / ezz(Lmax);
```

The differencing step is denoted as dX ($= \triangle$), and the simple Neumann boundary condition has been used. Although this matrix is neither unitary nor Hermitian, a canned routine is available for obtaining the eigenvectors and the eigenvalues of such odd-structured matrices. One good point about this matrix is that the eigenmode of the matrix [A] is the propagation constant itself. Programs including this code have been used to generate the figures in this article employing a *MatLab* function eig.

REFERENCES

[1] T. P. Sosnowski, "Polarization mode filters for integrated optics," *Opt. Commun.*, vol. 4, no. 6, pp. 408-412, 1972.

[2] M. Wakaki, Y. Komachi, H. Machida, and H. Kobayashi, "Fiber-optic polarizer using birefringent crystal as a cladding," *Appl. Opt.*, vol. 35, no. 15, pp. 2591-2594, 1996.

[3] G. K. Singh, V. K. Sharma, A. Kapoor, and K. N.

Tripathi, "Four layer polymeric mode polarization filter for integrated optics," *Optics & Laser Technology*, vol. 33, pp. 455-459, 2001.

[4] K. Liu, W. V. Sorin, and H. J. Shaw, "Single-mode-fiber evanescent polarizer/amplitude modulator using liquid crystals," *Opt. Lett.*, vol. 11, no. 3, pp. 180-182, 1986.

[5] R. A. Kashnow and C. R. Stein, "Total-reflection liquid-crystal electrooptic device," *App. Opt.*, vol. 12, no. 10, pp. 2309-2311, 1973.

[6] S. Wang, M. Shar, and J. D. Crow, "Studies of the use of gyrotropic and anisotropic materials for mode conversion in thin-film optical-waveguide applications," *J. Appl. Phys.*, vol. 43, no. 4, pp. 1861-1875, 1972.

[7] S. Yamamoto, Y. Koyamada, and T. Makimoto, "Normal-mode analysis of anisotropic and gyrotropic thin-film waveguides for integrated optics", *J. Appl. Phys.*, vol. 43, no. 12, pp. 5090-5097, 1972.

[8] J. Ćtyroký and M. Ćada, "Guided and semileaky modes in anisotropic optical waveguides of the $LiNbO_3$ type," *Opt. Commun.*, vol. 27, no. 3, pp. 353-357, 1978.

[9] K. Yamanouchi, T. Kamiya, and K. Shibayama, "New leaky surface waves in anisotropic metal-diffused optical waveguides," *IEEE Trans. Microwave Theory Tech.*, vol. 26, no. 4, pp. 298-305, 1978.

[10] S. K. Sheem, W. K. Burns, and A. F. Milton, "Leaky-mode propagation in Ti-diffused $LiNbO_3$ and $LiTaO_3$ waveguides," *Opt. Lett.*, vol. 3, no. 3, pp. 76-78, 1978.

[11] L. Torner, J. Recolons, and J. P. Torres, "Guided-to-leaky mode transition in uniaxial optical slab waveguides," *J. Lightwave Technol.*, vol. 11, no. 10, pp. 1592-1600, 1993.

[12] D. F. Nelson and J. McKenna, "Electromagnetic modes of anisotropic dielectric waveguides at p-n junctions," *J. Appl. Phys.*, vol. 38, no. 10, pp. 4057-4074, 1967.

[13] H. Kosaka, T. Kawashima, A. Tomita, M. Notomi, T. Tamamura, T. Sato, and S. Kawakami, "Superprism phenomena in photonic crystals: toward microscale lightwave circuits," *J. Lightwave Technol.*, vol. 17, no. 11, pp. 2032-2038, 1999.

[14] D. P. Gia Russo and J. H. Harris, "Wave propagation in anisotropic thin-film optical waveguides," *J. Opt. Soc. Am.*, vol. 63, no. 2, pp. 138-145, 1973.

[15] M. S. Kharusi, "Uniaxial and biaxial anisotropy in thin-film optical waveguides," *J. Opt. Soc. Am.*, vol. 64, no. 1, pp. 27-35, 1974.

[16] W. K. Burns and J. Warner, "Mode dispersion in uniaxial optical waveguides," *J. Opt. Soc. Am.*, vol. 64, no. 4, pp. 441-446, 1974.

[17] V. Ramaswamy, "Propagation in asymmetrical anisotropic film waveguides," *App. Opt.*, vol. 13, no. 6, pp. 1363-1371, 1974.

[18] D. Marcuse, "Modes of a symmetric slab optical waveguide in birefringent media-part I: optical axis not in plane of slab," *IEEE J. Quantum Electron.*, vol. 14, no. 10, pp. 736-741, 1978.

[19] D. Marcuse and I. P. Kaminow, "Modes of a symmetric slab optical waveguide in birefringent media, part II: slab with coplanar optical axis," *IEEE J. Quantum Electron.*, vol. 15, no. 2, pp. 92-101, 1979.

[20] E. A. Kolosovsky, D. V. Petrov, A. V. Tsarev, and I. B. Yakovkin, "An exact method for analysing light propagation in anisotropic inhomogeneous optical waveguides," *Opt. Commun.*, vol. 43, no. 1, pp. 21-25, 1982.

[21] A. Knoesen, T. K. Gayload, and M. G. Moharam, "Hybrid guided modes in uniaxial dielectric planar waveguides," *J. Lightwave Technol.*, vol. 6, no. 6, pp. 1083-1104, 1988.

[22] A. D'Orazio, M. De Sario, V. Petruzzelli, and F. Prudenzano, "Leaky mode propagation in planar multilayer birefringent waveguides: longitudinal dielectric tensor configuration," *J. Lightwave Technol.*, vol. 12, no. 3, pp. 453-462, 1994.

[23] T. A. Maldonado and T. K. Gayload, "Hybrid guided modes in biaxial planar waveguides," *J. Lightwave Technol.*, vol. 14, no. 3, pp. 486-499, 1996.

[24] D. V. Petrov and E. A. Kolosovsky, "Radiation modes of an anisotropic optical waveguide with arbitrary refractive index profile," *Opt. Commun.*, vol. 124, pp. 240-243, 1996.

[25] A. A. Romanenko, "Features of mode's characteristics of anisotropic planar optical waveguides in the vicinity of degeneration points," *Proc. SPIE*, vol. 4358, pp. 203-211, 2001.

[26] Q. Guo, Z. Shi, and W. Xu, "Modal fields of symmetric metal-clad planar uniaxial crystal waveguide," *Proc. SPIE*, vol. 4603, pp. 30-35, 2001.

[27] Y. Jeong and B. Lee, "Theory of electrically controllable long-period gratings built in liquid-crystal fibers", *Opt. Eng.*, vol. 40, no. 7, pp. 1227-1233, 2001.

[28] M. O. Vassell, "Structure of optical guided modes in planar multilayers of optically anisotropic materials," *J. Opt. Soc. Am.*, vol. 64, no. 2, pp. 166-173, 1974.

[29] P. Yeh, "Electromagnetic propagation in birefringent layered media," *J. Opt. Soc. Am.*, vol. 69, no. 5, pp. 742-756, 1979.

[30] L. M. Walpita, "Solutions for planar optical waveguide equations by selecting zero elements in a characteristic matrix," *J. Opt. Soc. Am. A*, vol. 2, no. 4, pp. 595-602, 1985.

[31] J. F. Offersgaard, "Waveguides formed by multiple layers of dielectric, semiconductor, or metallic media with optical loss and anisotropy," *J. Opt. Soc. Am. A*, vol. 12, no. 10, pp. 2122-2128, 1995.

[32] I. Hodgkinson, S. Kassam, J. Hazel, S. Cloughley, and Q. Wu, "Modal contours for biaxial thin-film waveguides," *Appl. Opt.*, vol. 35, no. 28, pp. 5569-5572, 1996.

[33] L. Thylen and D. Yevick, "Beam propagation method in anisotropic media," *Appl. Opt.*, vol. 21, no. 15, pp. 2751-2754, 1982.

[34] J. A. Fleck, Jr. and M. D. Feit, "Beam propagation method in uniaxial anisotropic media," *J. Opt. Soc. Am.*, vol. 73, no. 7, pp. 920-926, 1983.

[35] G. R. Hadley, "Wide-angle beam propagation using Pade approximant operators," *Opt. Lett.*, vol. 17, no. 20, pp. 1426-1428, 1992.

[36] C. L. Xu, W. P. Huang, J. Chrostowski, and S. K. Chaudhuri, "A full-vectorial beam propagation method for anisotropic waveguides," *J. Lightwave Technol.*, vol. 12, no. 11, pp. 1926-1931, 1994.

[37] S. V. Polstyanko and J. Lee, "H_1 (*curl*) tangential vector finite element method for modeling anisotropic

optical fibers," *J. Lightwave Technol.*, vol. 13, no. 11, pp. 2290-2295, 1995.

[38] Y. Tsuji, M. Koshiba, and N. Takimoto, "Finite element beam propagation method for anisotropic optical waveguides," *J. Lightwave Technol.*, vol. 17, no. 4, pp. 723-728, 1999.

[39] K. Saitoh and M. Koshiba, "Full-vectorial finite element beam propagation method with perfectly matched layers for anisotropic optical waveguides," *J. Lightwave Technol.*, vol. 19, no. 3, pp. 405-413, 2001.

[40] K. Saitoh and M. Koshiba, "Approximate scalar finite-element beam-propagation method with perfectly matched layers for anisotropic optical waveguides," *J. Lightwave Technol.*, vol.19, no. 5, pp. 786-792, 2001.

[41] A. Ciattoni, B. Crosignani, and P. Di Porto, "Vectorial theory of propagation in uniaxially anisotropic media," *J. Opt. Soc. Am. A*, vol. 18, no. 7, pp. 1656-1661, 2001.

[42] G. Kweon, S. Hwang-bo, and C. Kim, "Eigenmode of anisotropic planar waveguide," in Frontiers in Optics/ Laser Science XIX Conference, *Optical Society of America*, Tucson, Arizona, USA, MT62, 2003.

[43] D. W. Berreman, "Optics in stratified and anisotropic media: 4×4-matrix formulation," *J. Opt. Soc. Am.*, vol. 62, no. 4, pp. 502-510, 1972.

[44] P. J. Lin-Chung and S. Teitler, "4×4 matrix formalisms for optics in stratified anisotropic media," *J. Opt. Soc. Am. A*, vol. 1, no. 7, pp. 703-705, 1984.

[45] T. Tamir, Guided-Wave Optoelectronics, 2nd ed. (Springer-Verlag, Berlin, 1990), Chap. 2.

[46] G. Kweon, S. Hwang-bo, and C. Kim, "Eigenmode of planar magnetooptical waveguide," in *The 3rd International Conference on Advanced Materials and Devices, Korean Physical Society*, Jeju, Korea, DEV-P22, 2003.

[47] G. Kweon, S. Hwang-bo, and C. Kim, "Eigenmode of magnetooptical planar waveguide," *J. Korean Phys. Soc.*, vol. 45, no. 1, pp. 211-216, 2004.

[48] J. Berenger, "A perfectly matched layer for the absorption of electromagnetic waves," *J. Comput. Phys.*, vol. 114, pp. 185-200, 1994.